Temperature-Dependent Plasticity and Fracture Properties of Modern BCC Steels

Fuhui Shen[1,2(✉)], Hao Xu[1], Sebastian Münstermann[1], and Junhe Lian[2]

[1] Steel Institute, RWTH Aachen University, Intzestraße 1, 52072 Aachen, Germany
fuhui.shen@iehk.rwth-aachen.de

[2] Department of Mechanical Engineering, Aalto University, Otakaari 4, 02150 Espoo, Finland

Abstract. For some modern steels with a body-centered cubic (bcc) crystal structure, it is observed that both tensile strength and ductility are significantly improved with decreasing temperature, which motivates the exploration of the cryogenic formability and fracture properties of these materials. The temperature-dependent plasticity and fracture phenomena of a modern bainitic steels with the bcc structure have been investigated by performing a comprehensive experimental program and finite element simulations, covering a broad range of loading conditions. Uniaxial tensile tests have been performed at different temperatures along three loading directions. Tensile tests using flat specimens with various geometries, including shear, central hole and notched dog bone, have been performed along the rolling direction at room temperature and –196 °C. An advanced non-associated constitutive plasticity model is used to describe the temperature-dependent strength and hardening properties of the material. The local critical stress and strain variables extracted from finite element simulations of different fracture tests have been used to calibrate a unified fracture criterion, which considers the stress state dependence. The effects of temperature on the plasticity and stress state dependent fracture behavior of the modern bcc steels have been quantitatively determined.

Keywords: Anisotropy · Stress State · Cryogenic Fracture · FE Simulation

1 Introduction

Recent studies show that the formability of several aluminum alloys (with a face-centered cubic structure) at cryogenic temperatures is superior to room temperature, which motivates the exploration of the cryogenic formability of other metallic materials [1–3]. For metallic materials with a body-centered cubic (bcc) crystal structure, brittle fracture is typically observed in toughness tests when the testing temperature is below the ductile to brittle transition temperature. However, only a narrow range of stress states with high triaxiality is considered in the toughness tests. The fracture properties of modern bcc steels under low to moderate triaxiality conditions have not been fully explored. Recent studies show that significant amount of plasticity can occur in bainitic pipeline steels with a bcc structure at extremely low temperatures when the local stress triaxiality is below a threshold value [4, 5].

K. Mocellin et al. (Eds.): ICTP 2023, LNME, pp. 486–493, 2024.
https://doi.org/10.1007/978-3-031-40920-2_50

The effects of stress states on ductile fracture have been extensively investigated for various metallic materials [6–9]. Several uncoupled ductile fracture criteria have been proposed and applied to describe the stress state dependence of failure strain, which is typically formulated as the weight function of stress triaxiality and Lode angle parameter [10–12]. There are several successful applications of these criteria for the prediction of ductile fracture at elevated temperatures as well. However, the impacts of temperature on the plasticity and fracture properties of modern bcc steel over a wide range of stress states have rarely been investigated for temperatures lower than room temperature. For materials with anisotropic plasticity properties, different advanced constitutive models are available for the accurate description of plastic deformation at various temperatures [13–15]. Therefore, the temperature influence on the plasticity and fracture behavior of a modern bcc steel with anisotropic effects has been investigated under low to moderate triaxiality conditions at cryogenic temperatures.

2 Materials and Experiments

2.1 Materials and Testing Program

The plasticity and fracture properties of a modern bainitic steel have been investigated by performing tensile tests using different specimen geometries at room temperature and −196 °C under quasi-static conditions. The microstructure of the investigated bcc steel is shown in Fig. 1a. The plasticity of the material is characterized by performing uniaxial tensile tests using smooth dog bone (SDB) specimens along three different loading directions (00°, 45°, and 90° with respect to the rolling direction). The biaxial flow behavior is characterized by compression tests through the thickness direction. During uniaxial tensile tests at room temperature, the strains along both longitudinal and width directions have been measured to calculate the r-value. Tensile tests using fracture specimens, including notched dog bone (NDB), central hole (CH-R3) and shear (SH) geometries, have been performed along the rolling direction at room temperature and −196 °C. The gauge length of 40 mm is used for all fracture specimens. The detailed descriptions of the experimental setup are provided in previous studies [4, 16].

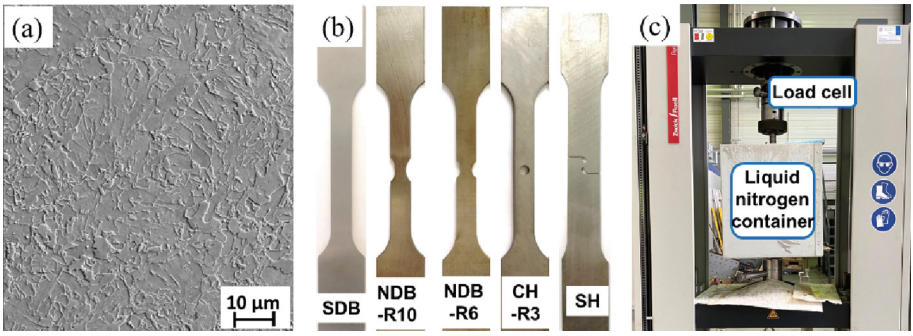

Fig. 1. Microstructure of the investigated material (a); Overview of all tensile specimens (b) and setup of the machine for tensile tests at −196 °C.

2.2 Experimental Results

The anisotropic engineering stress and strain curves obtained from uniaxial tensile tests at room temperature and −196 °C are shown in Fig. 2. Both yield strength and tensile strength are significantly increased at the cryogenic testing temperature than room temperature due to thermal softening effects. In addition, the tensile ductility at −196 °C is also significantly improved than at room temperature. The r-value along three loading directions has been measured continuously during tensile deformation at room temperature, as shown in Fig. 2d. In addition to the orientation-dependent flow stress, the anisotropic effects on the r-value are more pronounced. For instance, the r-value along 00° and 90° is lower than one. The r-value measured along different loading directions is also changing during plastic deformation.

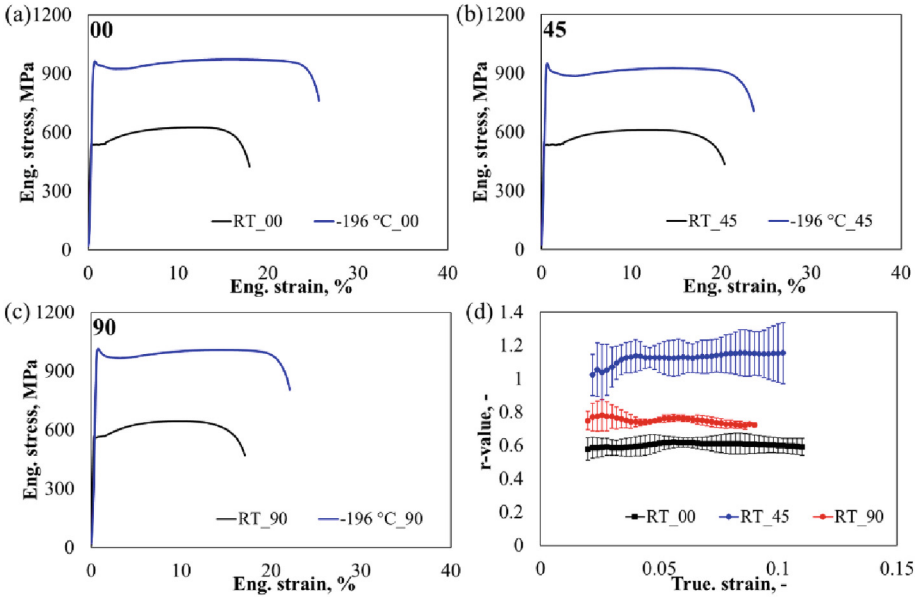

Fig. 2. Anisotropic uniaxial tensile properties of the investigated bcc steel at room temperature and −196 °C. Engineering stress and strain curves along (a) 00°, (b) 45°, and (c) 90°; (d) Evolution of r-value at room temperature.

Significant plastic deformation occurs in tensile tests using fracture specimens at both temperatures, as shown in the following section. However, the underlying failure mechanisms are different, depending on the loading stress states and temperature. For instance, shear failure occurs in the SH specimens at both room temperature and −196 °C. For the NDB specimens, cleavage fracture occurs after significant plastic deformation at −196 °C while ductile fracture takes place at room temperature.

3 Material Models

3.1 Plasticity Model

The non-associated flow rule has been adopted to overcome the drawback of the conventional Hill48 model, which provides limited accuracy in the simultaneous description of anisotropic strength and r-values [15, 17]. The features of anisotropic hardening and r-value evolution have been further considered in the evolving non-associated Hill48 (enHill48) model to improve the accuracy in describing the anisotropic plasticity [18]. The yield function f and flow potential g are described using separate equations.

$$f = \bar{\sigma}_\sigma(\boldsymbol{\sigma}|F_\sigma, G_\sigma, H_\sigma, L_\sigma, M_\sigma, N_\sigma) - \sigma_Y\left(\overline{\varepsilon}^p\right) \leq 0 \tag{1}$$

$$g = \bar{\sigma}_r(\boldsymbol{\sigma}|F_r, G_r, H_r, L_r, M_r, N_r) - \sigma_Y\left(\overline{\varepsilon}^p\right) \leq 0 \tag{2}$$

The same quadratic Hill48 equivalent stress $\bar{\sigma}(\boldsymbol{\sigma})$ is adopted in the yield function f and flow potential g, where the anisotropic parameters are calibrated independently. Anisotropic flow stress is used to calibrate parameters $(F_\sigma, G_\sigma, H_\sigma, N_\sigma)$ in yield function f while anisotropic r-values are used to determine parameters (F_r, G_r, H_r, N_r) in flow potential g.

$$\begin{aligned}\overline{\sigma}(\boldsymbol{\sigma}) = \{&\frac{1}{2}[F(\sigma_{22}-\sigma_{33})^2 + G(\sigma_{33}-\sigma_{11})^2 + H(\sigma_{11}-\sigma_{22})^2] \\ &+ L\sigma_{23}^2 + M\sigma_{13}^2 + N\sigma_{12}^2\}^{\frac{1}{2}}\end{aligned} \tag{3}$$

According to the non-associated flow rule, the equivalent plastic strain rate $\dot{\overline{\varepsilon}}^p$ is calculated in Eq. (4), where a correction factor is added to the typical non-negative plastic multiplier $\dot{\lambda}$.

$$\dot{\overline{\varepsilon}}^p = \dot{\lambda} \cdot \frac{\bar{\sigma}_r}{\bar{\sigma}_\sigma} \tag{4}$$

3.2 Fracture Criterion

The unified fracture criterion proposed by Shen et al., [4, 5] is used in this study, where the Bai-Wierzbicki [10] phenomenological expression of fracture initiation strain is adopted. The anisotropic damage mechanics model has been used to describe the fracture properties of high-strength bainitic steels at different temperatures [4, 16]. The general expression of stress state using stress triaxiality η and Lode angle parameter $\overline{\theta}$ is adopted in the fracture criterion, which are derived from stress invariants (I_1, J_2, J_3).

$$\eta = I_1/\sqrt{27 \cdot J_2} \tag{5}$$

$$\overline{\theta} = 1 - \frac{6}{\pi}\theta = 1 - \frac{2}{\pi}\cos^{-1}(\sqrt{27/4} \cdot J_3 \cdot {J_2}^{-3/2}) \tag{6}$$

The stress state effects on failure strain are quantified by a phenomenological function with four parameters ($C_{1\sim4}$) for proportional loading conditions according to Eq. (8). To consider the non-proportional loading effects, the average values of stress triaxiality and Lode angle parameter (η_{avg}, $\overline{\theta}_{\text{avg}}$) are used to describe the overall stress state. Fracture occurs when the fracture indicator I_{f} reaches the unity.

$$\overline{\varepsilon}_{\text{f}}\left(\eta,\overline{\theta}\right)=\left(C_1 exp^{-C_2\eta}-C_3 exp^{-C_4\eta}\right)\overline{\theta}^2+C_3 exp^{-C_4\eta} \tag{7}$$

$$\eta_{\text{avg}}=\frac{1}{\overline{\varepsilon}_{\text{f}}}\int_0^{\overline{\varepsilon}_{\text{f}}}\eta\, d\overline{\varepsilon}^{\text{p}},\ \overline{\theta}_{\text{avg}}=\frac{1}{\overline{\varepsilon}_{\text{f}}}\int_0^{\overline{\varepsilon}_{\text{f}}}\overline{\theta}\, d\overline{\varepsilon}^{\text{p}} \tag{8}$$

$$I_{\text{f}}=\int_0^{\overline{\varepsilon}^{\text{p}}}\frac{1}{\overline{\varepsilon}_{\text{f}}\left(\eta,\overline{\theta}\right)}d\overline{\varepsilon}^{\text{p}} \tag{9}$$

4 Simulation Results

4.1 Calibration of Plasticity Model

The orientation-dependent distribution of flow stress and r-value at the equivalent plastic strain of 0.04 can be well captured by the enHill48 plasticity model for both temperatures, as shown in Fig. 3a and Fig. 3b. Assuming the anisotropy of the investigated material is not affected by temperature, the r-value is considered to be independent of temperature [4, 19]. The anisotropic hardening behavior of the material is described by fitting the individual flow curves along 00°, 45°, 90° and the biaxial flow curve using the combined Swift-Voce function. The evolution of the r-value along three loading directions during plastic deformation is described using the Voce function. The fitting of the flow curve and r-value evolution function along the rolling direction is shown in Fig. 3c and Fig. 3d.

4.2 Critical Stress and Strain Values

Finite element simulations have been performed to extract the local critical stress and strain variables in different specimens. The material model is implemented as a user-defined VUMAT subroutine. Half-thickness models with solid elements have been used for all geometries during simulations using the ABAQUS/EXPLICIT software. The evolution of equivalent plastic strain with stress state variables in the critical element of CH-R3 and NDB-R6 specimens is demonstrated in Fig. 4 for both room temperature and −196 °C. Solid symbols represent the fracture point. It is observed that significant plastic deformation occurs at −196 °C during tensile tests along the rolling direction using these specimens. It can be seen that the fracture strain at room temperature is slightly higher than at −196 °C, indicating the temperature effects on fracture strain are not very pronounced under the investigated conditions.

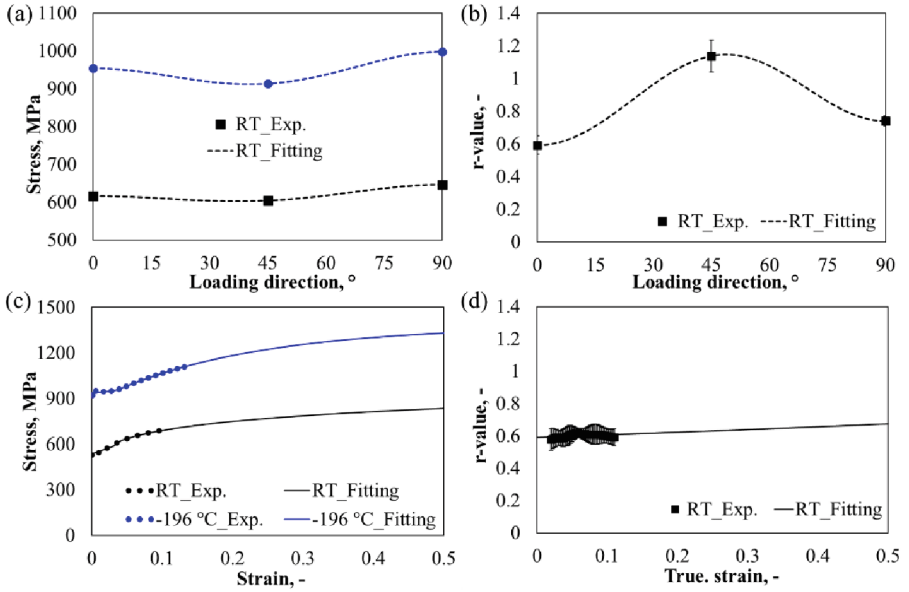

Fig. 3. Calibration of anisotropic plasticity model at room temperature and −196 °C: Anisotropic description of flow stress (a) and r-value (b) at the equivalent plastic strain of 0.04; Fitting of flow curve (c) and r-value evolution function (d) along the rolling direction.

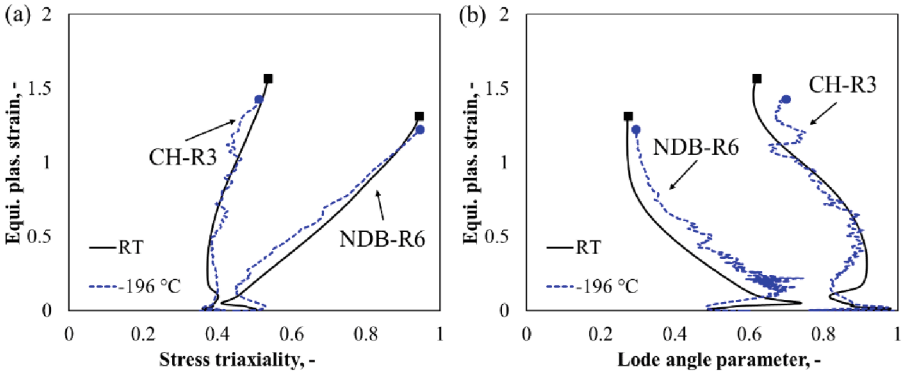

Fig. 4. The evolution of equivalent plastic strain with stress triaxiality (a) and Lode angle parameter (b) at critical position in CH-R3 and NDB-R6 specimens during tensile tests at room temperature and −196 °C along the rolling direction. Solid symbols represent fracture point.

4.3 Fracture Prediction

Considering the marginal effects of temperature on fracture strain, one set of fracture parameters ($C_{1\sim4}$) has been calibrated to describe the fracture behavior of the investigated bcc steel during tensile tests at room temperature and −196 °C along the rolling direction. The predicted force and displacement curves during tensile tests using CH-R3

and NDB-R6 specimens are compared with experimental results in Fig. 5. Based on good prediction accuracy, it can be concluded that the fracture behavior of the investigated bcc steel during tensile tests at room temperature and −196 °C can be well captured using one set of failure criterion under the considered loading conditions. Brittle fracture is typically observed in fracture toughness tests of engineering bcc materials at extremely low temperatures, which is mainly attributed to the high local triaxiality in the testing conditions. Recent studies show that significant plastic deformation can occur in bcc steels by delaying the cleavage fracture at cryogenic temperatures, far below the ductile to brittle transition temperature, if the local stress triaxiality is below a threshold value [4, 5].

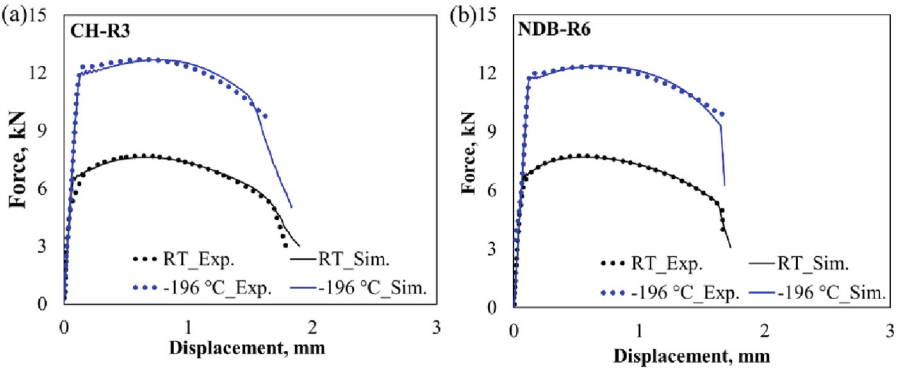

Fig. 5. Experimental and numerical results of force and displacement curves during tensile tests using CH-R3 (a) and NDB-R6 (b) specimens at room temperature and −196 °C along the rolling direction.

By comparing the fracture behavior at room temperature and −196 °C, it confirms that the local fracture strain of the investigated bcc steel at −196 °C is comparable to that of room temperature under the considered stress states below the threshold triaxiality, which is approximately 1 for the same grade of steel [4]. More systematic investigations should be performed to quantify the temperature effects on failure strain at other temperatures, particularly within the ductile to brittle transition region. However, these observations indicate that the local formability of modern bcc steels under low to moderate triaxiality conditions needs more exploration at cryogenic temperatures.

5 Conclusions

The effects of temperature on the plasticity and fracture properties of a bcc steel have been investigated by performing tensile tests using various specimen geometries at room temperature and −196 °C. The fracture properties during tensile tests at different temperatures have been simulated using an evolving plasticity model combined with a strain-based fracture criterion. The key findings are summarized as follows:

- Significant plasticity occurs at −196 °C in the investigated bcc steel during tensile tests using various specimen geometries, where the local triaxiality is below a threshold value.
- The temperature has weak impacts on the failure strain of the investigated bcc steel under the considered loading conditions.

References

1. Wang, X., Fan, X., Chen, X., Yuan, S.: Cryogenic deformation behavior of 6061 aluminum alloy tube under biaxial tension condition. J. Mater. Process. Technol. **303** (2022)
2. Yuan, S., Cheng, W., Liu, W.: Cryogenic formability of a solution-treated aluminum alloy sheet at low temperatures. J. Mater. Process. Technol. **298** (2021)
3. Liu, W., Hao, Y.: Damage and fracture prediction of 7075 high-strength aluminum alloy during cryogenic stamping process. Mech. Mater. **163** (2021)
4. Shen, F., Münstermann, S., Lian, J.: A unified fracture criterion considering stress state dependent transition of failure mechanisms in bcc steels at –196 °C. Int. J. Plast. **156** (2022)
5. Shen, F., Münstermann, S., Lian, J.: Cryogenic ductile and cleavage fracture of bcc metallic structures – influence of anisotropy and stress states. J. Mech. Phys. Solids, 105299 (2023)
6. Mu, L., Jia, Z., Ma, Z., Shen, F., Sun, Y., Zang, Y.: A theoretical prediction framework for the construction of a fracture forming limit curve accounting for fracture pattern transition. Int. J. Plast. **129** (2020)
7. Bao, Y., Wierzbicki, T.: On fracture locus in the equivalent strain and stress triaxiality space. Int. J. Mech. Sci. **46**(1), 81–98 (2004)
8. Shen, F., et al.: Local formability of medium-Mn steel. J. Mater. Process. Technol. **299** (2022)
9. Zhang, Y., et al.: Ductility prediction of HPDC aluminum alloy using a probabilistic ductile fracture model. Theor. Appl. Fract. Mech. **119** (2022)
10. Bai, Y., Wierzbicki, T.: A new model of metal plasticity and fracture with pressure and Lode dependence. Int. J. Plast. **24**(6), 1071–1096 (2008)
11. Lou, Y., Huh, H., Lim, S., Pack, K.: New ductile fracture criterion for prediction of fracture forming limit diagrams of sheet metals. Int. J. Solids Struct. **49**(25), 3605–3615 (2012)
12. Mohr, D., Marcadet, S.J.: Micromechanically-motivated phenomenological Hosford-Coulomb model for predicting ductile fracture initiation at low stress triaxialities. Int. J. Solids Struct. **67–68**, 40–55 (2015)
13. Barlat, F., Aretz, H., Yoon, J.W., Karabin, M.E., Brem, J.C., Dick, R.E.: Linear transfomation-based anisotropic yield functions. Int. J. Plast. **21**(5), 1009–1039 (2005)
14. Barlat, F., et al.: Plane stress yield function for aluminum alloy sheets—Part 1: theory. Int. J. Plast. **19**(9), 1297–1319 (2003)
15. Stoughton, T.B., Yoon, J.W.: Anisotropic hardening and non-associated flow in proportional loading of sheet metals. Int. J. Plast. **25**(9), 1777–1817 (2009)
16. Shen, F., Münstermann, S., Lian, J.: Investigation on the ductile fracture of high-strength pipeline steels using a partial anisotropic damage mechanics model. Eng. Fract. Mech. **227**, 106900 (2020)
17. Stoughton, T.B.: A non-associated flow rule for sheet metal forming. Int. J. Plast. **18**(5–6), 687–714 (2002)
18. Lian, J., et al.: An evolving non-associated Hill48 plasticity model accounting for anisotropic hardening and r-value evolution and its application to forming limit prediction. Int. J. Solids Struct. **151**, 20–44 (2018)
19. Shen, F., Münstermann, S., Lian, J.: An evolving plasticity model considering anisotropy, thermal softening and dynamic strain aging. Int. J. Plast **132**, 102747 (2020)